DESIGN AND ANALYSIS OF RELAY-ASSISTED MOLECULAR COMMUNICATION SYSTEMS

A PROJECT REPORT

Submitted in partial fulfillment of the requirements for the award of the degrees

of
BACHELOR OF TECHNOLOGY
in
ELECTRICAL ENGINEERING

Submitted by:
TADI RAVI TEJA REDDY

Guided by:
Dr. PRABHAT KUMAR UPADHYAY

INDIAN INSTITUTE OF TECHNOLOGY INDORE
NOVEMBER 2017

DECLARATION OF AUTHORSHIP

I hereby declare that the project entitled **"DESIGN AND ANALYSIS OF RELAY-ASSISTED MOLECULAR COMMUNICATION SYSTEMS**" submitted in partial fulfillment for the award of the degree of Bachelor of Technology in Electrical Engineering completed under the supervision of **Dr. Prabhat Kumar Upadhyay,** IIT Indore is an authentic work.

Further, I declare that I have not submitted this work for the award of any other degree elsewhere.

Signature and name of the student(s) with date

CERTIFICATE

It is certified that the above statement made by the students is correct to the best of my/our knowledge.

Signature of BTP Guide(s) with dates and their designation

Preface

This report on “Design and Analysis of Relay-Assisted Molecular Communication Systems” is prepared under the guidance of Dr. Prabhat Kumar Upadhyay.

Through this report we have tried to give a detailed analysis of joint optimization in a relay-assisted molecular communication system for improving the error performance of the system. The parameters under investigation are decision thresholds, relay positioning and messenger molecules distribution parameter.

TADI RAVI TEJA REDDY
B.Tech. IV Year
Discipline of Electrical Engineering
IIT Indore

DESIGN AND ANALYSIS OF RELAY-ASSISTED MOLECULAR COMMUNICATION SYSTEMS

“ Research shows that the climate of an organization influences an individual’s contribution far more than the individual himself ”

ABSTRACT

The error performance of a relay assisted diffusion-based molecular communication system relies on detection thresholds, the position of relay, and number of messenger molecules allocated to each link. Arbitrary values of these parameters would increase the error probability and render the system useless. Hence, the appropriate values of these parameters are required to be determined to minimize the probability of error. In this project report, we investigate two problem sets with different parameter constraints. First, we fix the position of relay and number of molecules allocated to the relay and receiver and propose a new approach that yields optimal value for decision threshold. Second, we find the optimal relay position as well as the optimal amount of molecules allocated to each of the transmitting nodes. To solve this optimization problem, we propose an iterative algorithm based on the block coordinate descent algorithm and study its convergence behavior. Numerical results show that our analyses help in designing a reliable relay based molecular communication network.

ACKNOWLEDGEMENTS

I would like to express my deepest gratitude to my advisor **Dr. Prabhat Kumar Upadhyay** for his invaluable guidance, patience, and support. I have learned a lot from him, in problem-solving and conducting meaningful research and giving clear presentations. It is absolutely amazing how closely he has worked with me on problems, allowing me time to make mistakes and learn from them. He has always been approachable, friendly, responsive and enthusiastic towards working on problems, which kept me motivated. I feel very fortunate to have been given an opportunity to work on hard, conceptual problems that are also relevant. Also, I am extremely grateful for the collaborations in this work with Ph.D. scholar **Satish**. Satish is a great researcher and instrumental in the completion of this project. I would also like to thank my committee members for their participation in my BTP presentations.

Finally, I would also like to express my gratitude to my family, for providing unconditional support to pursue my academic goals. Their support and values, helped me go through some tough times. Their insistence on sincerity and dedication has been instrumental in helping me achieve my goals.

Contents

List of Figures

Abbreviations

RF	**R**adio **F**requency
MC	**M**olecular **C**ommunication
DbMC	**D**iffusion-**b**ased **M**olecular **C**ommunication
AF	**A**mplify-and-**F**orward
DF	**D**ecode-and-**F**orward
ML	**M**aximum **L**ikelihood
KKT	**K**arush-**K**uhn-**T**ucker
BCDA	**B**lock **C**ordinate **D**escent **A**lgorithm

To my parents and grandparents.

Chapter 1

Introduction

1.1 Background

Communication systems are ubiquitous. These systems enable people to share information with others, these types of systems can be classified into two categories, Natural and synthetic. Many forms of synthetic communication are digital, where the message produced by the information source is converted into a sequence of binary digits and transmitted [1]. Natural communication is not just restricted to the exchange of information between humans. Animals can also communicate via chemical signaling (e.g., Pheromones), visual signals (e.g., fireflies), sound (e.g., whales can communicate over hundreds of kilometers), tactile signaling (e.g., honeybee dancing), and electric signals (e.g., some species of fish) [2]. Cell-cell communication is a widespread phenomenon in nature, ranging from bacterial quorum sensing and fungal pheromone communication to cellular crosstalk in multicellular eukaryotes.

A synthetic network at the scale of biological cells is of interest, as it could operate in a biological environment, in small industrial devices, or even in the air. This kind of network, where the communicating devices have functional components that are on the order of nanometers in size, has been defined as a nanonetwork [3]. These communication modes offer the possibility to control the behavior of an entire community by modifying the performance of individual cells in specific ways. The interest in nanonetworks is for applications in a diverse number of fields, including biological engineering, healthcare, environmental monitoring, and manufacturing. The functionality of nanoscale devices would critically depend on the ability to communicate since it is anticipated that any single device would be too small to have significant processing capacity. Thus, the fundamental challenge in the implementation of nanonetworks is designing appropriate mechanisms that enable communication between the devices in this scale.

Conventional synthetic strategies for ad-hoc communication between mobile devices (radio frequency (RF)) transmission, might be unsafe or infeasible in the environments where nanonetworks are to be deployed, such as in biological systems. One of the most promising approaches is to gain inspiration from how natural communication occurs in these environments and determine whether natural mechanisms can be adapted for use in synthetic networks.

Molecular communication (MC) is a new communication paradigm using molecules as a communication carrier. In molecular communication, information is encoded onto molecules at senders and the molecules propagate to receivers. The receivers, upon receiving the molecules, decode the encoded information and react biochemically. Molecular communication provides means to deliver molecules to destinations and allows biological and artificially-created components to communicate with each other. Molecular communication has potentialities to enable future healthcare applications as it is ubiquitous in biological systems [4].

The MC method that has attracted the most attention from the communications research community is free diffusion [5]. Prior experimental work has already developed a functioning macroscale prototype of a system using diffusive communication with flow [6]. Diffusion can be modeled as a random walk where molecules collide with other molecules in the propagation environment. Its primary advantage is its simplicity since molecules that are released by a transmitter can freely diffuse away without any external energy or infrastructure requirements. The lack of infrastructure between devices means that diffusion is appropriate for the formation of ad hoc networks between mobile devices.

Diffusion can be very fast over short distances, and is a common means of communication in nature; many cellular processes rely on diffusion for limited quantities of molecules to efficiently propagate both within and between cells [7]. However, this strategy faces two important problems, First, the average distance traveled by a diffusing molecule is proportional to the square root of the time that it takes to diffuse. So, molecular communication systems have to deal with increasingly longer propagation times as the receiver is placed further away. Second, there is a lack of control over where each molecule goes, so a large number of molecules are required to ensure that a sufficient number arrive at the receiver instead of just diffusing away.

1.2 Motivation

Despite the advantages of the diffusion-based molecular communication (DbMC), it has a limited communication range due to the attenuation of the molecules concentration. One approach to alleviate this problem is to deploy cooperative relay nanomachines between transmitter and receiver nanomachines [8]. The cooperation protocol used by such relay nanomachines can

be either amplify-and-forward (AF) [9] [10] or decode-and-forward (DF) protocol [10] [11]. In this project report, we consider a DF relay-aided DbMC system and investigate the following important communication parameters for minimizing the error performance of the system:

1. Detection thresholds at relay and destination node.
2. Location of the relay node.
3. Distribution of messenger molecules between the source and relay node.

These factors play a crucial role in determining the error performance and the futuristic design of the system. Owing to the limited computational capability of nanomachines, a simple detector for DbMC systems has been introduced in [12] that compares the molecular count over a period of time (i.e., energy) with a pre-determined threshold. The performance of such a detector depends on the chosen value of the detection threshold. As such, decreasing detection threshold increases the probability of false alarm, whereas increasing detection threshold increases the probability of miss detection. The relay position and distribution of messenger molecules is another important aspect in determining the error performance of MC system [13], for example, if the relay is placed arbitrarily without taking into account the distribution of allocated molecules for message transmission, it might decrease the error probability in one of the links, but it will certainly increase the error probability of the other link, affecting the overall error performance of the system.

In some scenarios of DbMC, such as an intra-body network, transmitter and receiver nanomachines (nodes) are suspended in a fluidic medium where they are likely to be mobile and their movement are usually modeled as the Brownian motion [14]. But if both the transmitter and the receiver are anchored to larger objects, they are immobilized in the medium and it is possible to have both of them at fixed locations or to have a fixed distance between them [15]. The immobilization of the nodes for a time that is sufficient to establish a reliable communication makes the network well suited for applications requiring fixed nanomachines. For example, some nanomedical applications may necessitate a predefined network topology in which the communicating nodes must be statically deployed on some critical points inside the human body to perform their tasks (e.g., early detection of heart attack). In such applications, all communication parameters must be regulated with respect to the predefined topology to achieve minimum network error [16]. A few other applications include target detection by a static bionanosensor network and detection of targets sites (disease sites, pathogens, or infectious microorganisms) [17].

Research is needed to develop optimization techniques for DbMC systems that optimize parameters based on predefined topology. In this report, we develop optimization techniques for the following two problem sets:

1. Detection thresholds at relay and destination node.

2. Location of the relay node and distribution of messenger molecules.

These problem sets correspond to a large number of practical scenarios, the main objective of this report is to address the aforementioned optimization problems.

The remainder of this project report is structured as follows. In Chapter 2, the system model is described and error performance analysis is carried out. Chapter 3 presents the proposed optimization problems and their solutions. Chapter 4 demonstrates the numerical and simulation results. Finally, Chapter 5 draws the conclusion.

Chapter 2

Channel Model and Error Performance Analysis

2.1 System Model

The performance analysis of a communication system requires a detailed understanding of the propagation environment and the impact of associated parameters. For DbMC, to understand the behavior of molecules we need to investigate them from the time they are released by the transmitter and until they are removed from the environment. Diffusion being an imperfect process is best described by an expected channel impulse response, i.e., the number of molecules expected at a receiver when messenger molecules are released by a transmitter. The expected channel impulse response is a function of the parameters and geometry of the diffusive environment, the distance from the transmitter to the receiver, the diffusion coefficient of the molecules, and the time elapsed since the molecules were released. Chemical reactions that have the molecules of interest as a product or reactant and other sources of similar molecules that are not the intended transmitter, can also impact the status of diffusing molecules and hence the channel impulse response.

We consider a DbMC system wherein a transmitter nanomachine (node S) communicates molecular signal to a receiver nanomachine (node D) with the assistance of a linearly placed relay nanomachine (node R) via unbounded three-dimensional diffusive medium having uniform temperature and viscosity. Intermediate node R is placed at distance $d_{mn} + r$ from end nodes, where d_{mn} is the distance from center of transmitting node $m \in \{\mathrm{S}, \mathrm{R}\}$ to the closest point on the surface of respective receiving node $n \in \{\mathrm{R}, \mathrm{D}\}$ and r is the radius of fully absorbing [18] spherical nodes R and D. Moreover, node R utilizes full-duplex transmission protocol with DF strategy. We assume that relay R detects type A molecules released by node S and emits type B molecules to be detected by node D. Nodes D and R are transparent to molecules A and B, respectively.

Further, we make use of on-off keying modulation wherein nodes S and R respectively release N_A and N_B number of molecules at the beginning of the symbol duration T to convey the information bit 1 and no molecules for information bit 0. These molecules propagate through the diffusive channel and may degrade [19] before hitting the receiver boundary. All nodes are assumed to be synchronized in time (e.g., using strategy described in [20]) and remain static during the symbol duration.

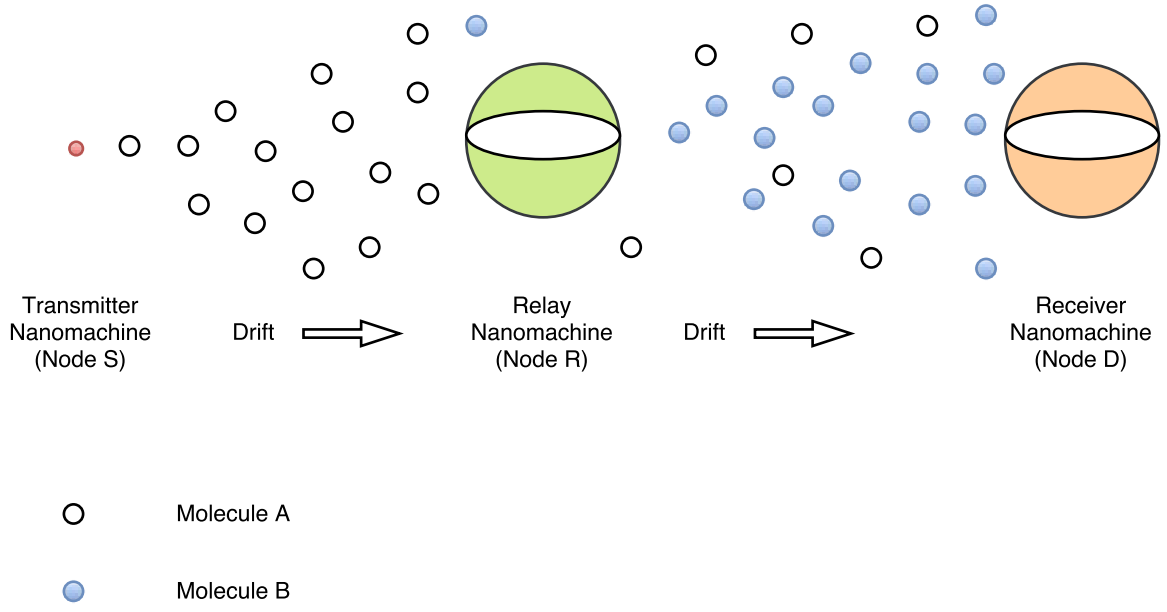

FIGURE 2.1: A relay-assisted diffusion-based molecular communication system

2.2 Channel Impulse response

The first hitting probability function for a spherical absorbing receiver in a three-dimensional molecular degraded diffusive channel, between nodes m and n, is derived in [19] as

$$h_f^{mn}(t) = \frac{r}{d_{mn}+r}\frac{d_{mn}}{\sqrt{4\pi D_f t^3}}\exp\left[-\frac{d_{mn}^2}{4D_f t}-\lambda t\right], \tag{2.1}$$

where λ is the rate of molecular degradation and D_f is the diffusion coefficient of type $f \in \{A, B\}$ molecules in the given medium. Consequently, the probability that a molecule transmitted by

node m in the ith previous symbol duration arrives at node n in the current symbol duration is given as

$$P_{i,f}^{mn} = H_f^{mn}\big((i+1)T\big) - H_f^{mn}\big(iT\big), \tag{2.2}$$

where

$$H_f^{mn}(t) = \frac{r}{2(d_{mn}+r)}\Bigg[\exp\Big(d_{mn}\sqrt{\lambda/D_f}\Big)\operatorname{erfc}\Big(d_{mn}/\sqrt{4D_f t}+\sqrt{\lambda t}\Big) + \exp\Big(-d_{mn}\sqrt{\lambda/D_f}\Big)\operatorname{erfc}\Big(d_{mn}/\sqrt{4D_f t}-\sqrt{\lambda t}\Big)\Bigg] \tag{2.3}$$

is the fraction of molecules released by node m that are absorbed at node n before degradation within time t.

2.3 Error Performance Analysis

In addition to the residual molecules from previous transmissions, the molecular signal is also affected by the molecules emitted from other nanomachines present in the diffusive medium and the counting error at the reception node. As such, the total number of molecules received at node n in jth symbol duration can be expressed as

$$W_f^{mn}[j] = U_f^{mn}[j] + N_{r,f}^{mn}[j] + N_{o,f}^{mn}[j] + N_{c,f}^{mn}[j], \tag{2.4}$$

where $U_f^{mn}[j]$ and $N_{r,f}^{mn}[j]$ represent binomial distributed received molecular counts from current and previous transmissions respectively. For large N_f, the distributions of $U_f^{mn}[j]$ and $N_{r,f}^{mn}[j]$ can be approximated[1] by Gaussian distributions [13]

$$U_f^{mn}[j] = \mathcal{N}\big(a_j^m N_f P_{0,f}^{mn}, a_j^m N_f P_{0,f}^{mn}(1-P_{0,f}^{mn})\big) \tag{2.5}$$

$$N_{r,f}^{mn}[j] = \sum_{i=1}^{I} \mathcal{N}\big(a_{j-i}^m N_f P_{i,f}^{mn}, a_{j-i}^m N_f P_{i,f}^{mn}(1-P_{i,f}^{mn})\big) \tag{2.6}$$

[1] Although Poisson distribution could be a better approximation for the received number of molecules in DbMC systems with molecular degradation [19], we use Gaussian approximation since relay deployment inevitably increases the received number of molecules.

where a_j^m and a_{j-i}^m are respectively jth current and $(j-i)$th previous transmitted bits by node m, and I denotes the number of previous bits. Moreover, $N_{o,f}^{mn}[j]$ represents the number of molecules received from other nanomachines present in the diffusive medium and $N_{c,f}^{mn}[j]$ represents the counting error at node n, following the distributions $\mathcal{N}(\mu_{no}^{mn}, \sigma_{no}^{2,mn})$ and $\mathcal{N}(0, \sigma_{nc}^{2,mn})$ respectively [13].

The mean and variance values mentioned above are given by

$$\mu_0^{\mathrm{SR}} = \frac{N_A}{2} \sum_{i=1}^{I} P_{i,\mathrm{A}}^{\mathrm{SR}} + \mu_{\mathrm{no}}^{\mathrm{SR}} \tag{2.7}$$

$$\mu_1^{\mathrm{SR}} = \frac{N_A}{2} \sum_{i=1}^{I} P_{i,\mathrm{A}}^{\mathrm{SR}} + N_A P_{0,\mathrm{A}}^{\mathrm{SR}} + \mu_{\mathrm{no}}^{\mathrm{SR}} \tag{2.8}$$

$$\sigma_0^{2,\mathrm{SR}} = \frac{N_A}{2} \sum_{i=1}^{I} P_{i,\mathrm{A}}^{\mathrm{SR}}(1 - P_{i,\mathrm{A}}^{\mathrm{SR}}) + \frac{N_A^2}{4} \sum_{i=1}^{I} (P_{i,\mathrm{A}}^{\mathrm{SR}})^2 + \sigma_{\mathrm{no}}^{2,\mathrm{SR}} + \mu_0^{\mathrm{SR}} \tag{2.9}$$

$$\sigma_1^{2,\mathrm{SR}} = N_A P_{0,\mathrm{A}}^{\mathrm{SR}}(1 - P_{0,\mathrm{A}}^{\mathrm{SR}}) + \frac{N_A}{2} \sum_{i=1}^{I} P_{i,\mathrm{A}}^{\mathrm{SR}}(1 - P_{i,\mathrm{A}}^{\mathrm{SR}}) + \frac{N_A^2}{4} \sum_{i=1}^{I} (P_{i,\mathrm{A}}^{\mathrm{SR}})^2 + \sigma_{\mathrm{no}}^{2,\mathrm{SR}} + \mu_1^{\mathrm{SR}} \tag{2.10}$$

μ_0^{RD}, μ_1^{RD}, $\sigma_0^{2,\mathrm{RD}}$ and $\sigma_1^{2,\mathrm{RD}}$ are calculated likewise.

we now analyze the expected error probability of the considered DbMC system. Error occurs if the detection is erroneous at either node R or node D. Consequently, the error probability for the jth bit can be calculated as

$$\begin{aligned} P_e[j] =& \Pr(a_j^{\mathrm{S}} = 1) \times \Pr(\hat{a}_{j+1}^{\mathrm{D}} = 0 \mid a_j^{\mathrm{S}} = 1) \\ &+ \Pr(a_j^{\mathrm{S}} = 0) \times \Pr(\hat{a}_{j+1}^{\mathrm{D}} = 1 \mid a_j^{\mathrm{S}} = 0) \end{aligned} \tag{2.11}$$

and is given by

$$\begin{aligned} P_e[j] = \frac{1}{2} + \frac{1}{2} \left[Q\left(\frac{\eta_{\mathrm{R}} - \mu_0^{\mathrm{SR}}}{\sqrt{\sigma_0^{2,\mathrm{SR}}}} \right) - Q\left(\frac{\eta_{\mathrm{R}} - \mu_1^{\mathrm{SR}}}{\sqrt{\sigma_1^{2,\mathrm{SR}}}} \right) \right] \\ \times \left[Q\left(\frac{\eta_{\mathrm{D}} - \mu_1^{\mathrm{RD}}}{\sqrt{\sigma_1^{2,\mathrm{RD}}}} \right) - Q\left(\frac{\eta_{\mathrm{D}} - \mu_0^{\mathrm{RD}}}{\sqrt{\sigma_0^{2,\mathrm{RD}}}} \right) \right], \end{aligned} \tag{2.12}$$

assuming equally probable binary bits, where $\hat{a}_{j+1}^{\mathrm{D}}$ is the information bit detected by node D in the $(j+1)$th symbol duration

where

$$Q(x) = \frac{1}{\sqrt{2\pi}} \int_{x}^{\infty} \exp(-\frac{x^2}{2}) \mathrm{d}x \tag{2.13}$$

In the next chapter, we investigate the various parameters for optimizing the error probability and propose their solutions.

Chapter 3

Problem Formulation and Parameter Optimization

3.1 Problem Formulation

In the previous chapter, we derived a closed-form expression for the bit error probability performance of the proposed detection scheme given by:

$$P_e[j] = \frac{1}{2} + \frac{1}{2}\left[Q\left(\frac{\eta_{\mathrm{R}} - \mu_0^{\mathrm{SR}}}{\sqrt{\sigma_0^{2,\mathrm{SR}}}}\right) - Q\left(\frac{\eta_{\mathrm{R}} - \mu_1^{\mathrm{SR}}}{\sqrt{\sigma_1^{2,\mathrm{SR}}}}\right)\right] \times \left[Q\left(\frac{\eta_{\mathrm{D}} - \mu_1^{\mathrm{RD}}}{\sqrt{\sigma_1^{2,\mathrm{RD}}}}\right) - Q\left(\frac{\eta_{\mathrm{D}} - \mu_0^{\mathrm{RD}}}{\sqrt{\sigma_0^{2,\mathrm{RD}}}}\right)\right] \tag{3.1}$$

It is clear from (3.1) that the bit error probability of the network depends on the mean and variance values of the energy received from S-D and R-D links, and the detection threshold at relay R and destination D. As discussed in Chapter 1, owing to the limited memory and computational capabilities of the nanoreceiver it would be practically feasible to only consider two parameters at a time for optimization. If the number of molecules released by nodes S and R, i.e., Q_A and Q_B, and the position of relay is fixed, the performance of a molecular signal detector relies on the selected value of the detection threshold. In fact, arbitrary choice of detection threshold would increase either the probability of miss detection or the probability of false alarm. Thereby, an appropriate value of detection threshold is required in order to optimize the error performance of a DbMC system.

Similarly, the bit error probability of the network depends on the mean and variance values of the energy received from S-D and R-D links. If the thresholds at both, the relay and destination are fixed, then changing the location of the relay node and the number of molecules released

by nodes S and R, leads to a change in the mean and variance values due to change in the probability of molecules being observed. Since the performance of the cooperative MC networks strongly depends on the relay position [13], an important problem is to determine the optimum location of the relay node in order to achieve the minimum network error. The distribution of messenger molecules to each of the links is equally important for a fixed value of decision threshold. If the budget is much higher (lower) then the optimized value it would increase the probability of false alarm (probability of miss detection). In MC systems the power consumed is directly proportional to the number of messenger molecules transmitted, thus, to account for the constraint in the consumption of power, we assume that the total number of messenger molecules is fixed. The optimum relay position is on the straight line connecting the source and the destination nodes. This is because if the relay node is located at other positions, then its distance to both the source and the destination nodes are always larger than their corresponding projections on the straight line connecting the source and the destination nodes which leads to an increase in the bit error probability.

In this report we consider two problem sets:

1. Optimization of error probability with respect to detection thresholds at relay and receiver (η_{R} and η_{D}).
2. Optimization of error probability with respect to relay position and messenger molecules distribution parameter.

3.2 Decision Thresholds Optimization

There are two thresholds in the error probability equation, one associated to the relay η_{R} and the other to destination η_{D}. In this case, we fix the relay location and the messenger molecules at source and relay. First, to understand the effectiveness of our approach, we will optimize the error probability with respect to the threshold at a single node. To illustrate this, we will fix the threshold for the relay and apply our approach for the destination nanomachine receiver. The detection threshold at the relay can be calculated using Maximum Likelihood (ML) principle.

$$\eta_{\mathrm{R}} = \left\lfloor (\sqrt{\alpha^2 + 2\beta ln(\gamma)} - \alpha)/\beta \right\rceil \tag{3.2}$$

where $ln(\cdot)$ is the natural logarithm, $\lfloor \cdot \rceil$ is the nearest integer function (number of molecules cannot be a fraction, it has to be an integer), $\alpha = (\mu_1^{\mathrm{SR}}/\sigma_1^{2,\mathrm{SR}}) - (\mu_0^{\mathrm{SR}}/\sigma_0^{2,\mathrm{SR}})$, $\beta = (1/\sigma_0^{2,\mathrm{SR}}) - (1/\sigma_1^{2,\mathrm{SR}})$ and $\gamma = \left(\sqrt{\sigma_1^{2,\mathrm{SR}}/\sigma_0^{2,\mathrm{SR}}}\right) \times \exp\left(0.5(\mu_1^{\mathrm{SR}})^2/\sigma_1^{2,\mathrm{SR}} - 0.5(\mu_0^{\mathrm{SR}})^2/\sigma_0^{2,\mathrm{SR}}\right)$.

The error probability is now a function of decision threshold η_{D}. Hence, we seek the optimal detection threshold, $\eta_{\mathrm{D}}^{\mathrm{opt}}$, that minimizes (3.1). To this end, we impose constraints on η_{D} so as to make $P_e[j]$ convex [21] with respect to η_{D}.

In order to make $P_e[j]$ convex with respect to η_{D}, the convex constraints can be imposed as

$$(\mu_0^{\mathrm{RD}} - \eta_{\mathrm{D}}) \leq 0 \quad \text{and } (-\mu_1^{\mathrm{RD}} + \eta_{\mathrm{D}}) \leq 0. \tag{3.3}$$

Since the decision threshold at relay is dealt with, we can optimize the decision threshold at the destination. One can prove the convexity of $P_e[j]$ by showing that its second-order derivative with respect to η_{D} is non-negative [22]. We evaluate the second order derivative of $P_e[j]$ as

$$\frac{\partial^2 P_e[j]}{\partial \eta_{\mathrm{D}}^2} = \frac{0.5\Lambda}{\sqrt{2\pi}} \left[\frac{(\eta_{\mathrm{D}} - \mu_1^{\mathrm{RD}})\,\Phi}{\left(\sigma_1^{2,\mathrm{RD}}\right)^{3/2}} - \frac{(\eta_{\mathrm{D}} - \mu_0^{\mathrm{RD}})\,\Psi}{\left(\sigma_0^{2,\mathrm{RD}}\right)^{3/2}} \right], \tag{3.4}$$

where $\Lambda = Q\big((\eta_{\mathrm{R}} - \mu_0^{\mathrm{SR}})/\sqrt{\sigma_0^{2,\mathrm{SR}}}\big) - Q\big((\eta_{\mathrm{R}} - \mu_1^{\mathrm{SR}})/\sqrt{\sigma_1^{2,\mathrm{SR}}}\big)$, $\Phi = \exp\big(-(\eta_{\mathrm{D}} - \mu_1^{\mathrm{RD}})^2/2\sigma_1^{2,\mathrm{RD}}\big)$ and $\Psi = \exp\big(-(\eta_{\mathrm{D}} - \mu_0^{\mathrm{RD}})^2/2\sigma_0^{2,\mathrm{RD}}\big)$. Since Φ and Ψ always return positive value irrespective of their argument and Λ is always negative, (3.4) is always nonnegative if constraint (3.3) is applied.

Now, we formulate the convex optimization problem for the proposed system as

$$\begin{aligned} \min_{\eta_{\mathrm{D}}} \quad & P_e[j] \\ \text{s.t.} \quad & (3.3). \end{aligned} \tag{3.5}$$

Then, we rewrite problem (3.9), making the inequality constraints implicit in the objective by using logarithmic barrier function followed by writing Karush-Kuhn-Tucker (KKT) interpretation of centrality condition:

$$\begin{cases} 0.5\Lambda\big(\Psi/\sqrt{2\pi\sigma_0^{2,\mathrm{RD}}} - \Phi/\sqrt{2\pi\sigma_1^{2,\mathrm{RD}}}\big) - \lambda_1 + \lambda_2 = 0 \\ -\lambda_1\big(\mu_0^{\mathrm{RD}} - \eta_{\mathrm{D}}\big) = \frac{1}{\varepsilon} \\ -\lambda_2\big(-\mu_1^{\mathrm{RD}} + \eta_{\mathrm{D}}\big) = \frac{1}{\varepsilon}, \end{cases} \tag{3.6}$$

where λ_1 and λ_2 are KKT multipliers, and $\varepsilon > 0$ is a parameter that sets the accuracy of the barrier approximation.

Further, on eliminating λ_1 and λ_2 from the modified KKT equations (3.6), we get

$$\begin{aligned} &0.5\Lambda\big(\Psi/\sqrt{2\pi\sigma_0^{2,\mathrm{RD}}} - \Phi/\sqrt{2\pi\sigma_1^{2,\mathrm{RD}}}\big) \\ &+1/\big(\varepsilon(\mu_0^{\mathrm{RD}} - \eta_{\mathrm{D}})\big) + 1/\big(\varepsilon(\mu_1^{\mathrm{RD}} - \eta_{\mathrm{D}})\big) = 0. \end{aligned} \tag{3.7}$$

Eventually, using Newton Raphson method, as in [23], approximate optimal detection threshold or suboptimal detection threshold after $(k+1)$th iterations is given as

$$\begin{aligned}\eta_{\mathrm{D}}^{k+1} &= \eta_{\mathrm{D}}^{k} - \frac{\frac{0.5\Lambda\Psi^k}{\sqrt{2\pi\sigma_0^{2,\mathrm{RD}}}} - \frac{0.5\Lambda\Phi^k}{\sqrt{2\pi\sigma_1^{2,\mathrm{RD}}}} + \frac{1}{\varepsilon}\left(\frac{1}{\Theta^k} + \frac{1}{\Xi^k}\right)}{\frac{0.5\Theta^k\Lambda\Psi^k}{\sqrt{2\pi}(\sigma_0^{2,\mathrm{RD}})^{3/2}} - \frac{0.5\Xi^k\Lambda\Phi^k}{\sqrt{2\pi}(\sigma_1^{2,\mathrm{RD}})^{3/2}} + \frac{1}{\varepsilon(\Theta^k)^2} + \frac{1}{\varepsilon(\Xi^k)^2}} \\ &= \eta_{\mathrm{D}}^{\mathrm{Sopt}}, \end{aligned} \tag{3.8}$$

where Ψ^k and Φ^k are respectively given by expressions for Ψ and Φ with η_{D} replaced by η_{D}^k, $\Theta^k = (\mu_0^{\mathrm{RD}} - \eta_{\mathrm{D}}^k)$, and $\Xi^k = (\mu_1^{\mathrm{RD}} - \eta_{\mathrm{D}}^k)$.

The applied logarithmic barrier grows without bound irrespective of the value of ε, if either of the constraints in (3.3) tends to 0. Moreover, value obtained from (3.8) is no more than $2/\varepsilon-$suboptimal and converges to optimal point, $\eta_{\mathrm{D}}^{\mathrm{opt}}$, as ε grows. Furthermore, one can get optimal solution by rounding $\eta_{\mathrm{D}}^{\mathrm{Sopt}}$, corresponding to appropriate ε, to the nearest integer. This is further illustrated through Figs. 4.1-4.3 in the next chapter. We have published these results in [24].

Since our primary goal is joint-optimization with respect to both the detection thresholds, we formulate the optimization problem as

$$\min_{\eta_{\mathrm{D}},\eta_{\mathrm{R}}} \quad P_e[j], \tag{3.9}$$

A careful inspection of (3.1) reveals that the error probability is composed of two parts:

$$Q\left(\frac{\eta_{\mathrm{R}} - \mu_0^{\mathrm{SR}}}{\sqrt{\sigma_0^{2,\mathrm{SR}}}}\right) - Q\left(\frac{\eta_{\mathrm{R}} - \mu_1^{\mathrm{SR}}}{\sqrt{\sigma_1^{2,\mathrm{SR}}}}\right) \tag{3.10}$$

and

$$Q\left(\frac{\eta_{\mathrm{D}} - \mu_1^{\mathrm{RD}}}{\sqrt{\sigma_1^{2,\mathrm{RD}}}}\right) - Q\left(\frac{\eta_{\mathrm{D}} - \mu_0^{\mathrm{RD}}}{\sqrt{\sigma_0^{2,\mathrm{RD}}}}\right) \tag{3.11}$$

Since the relay distance and number of molecules for transmission are fixed, each one of them is independent of the other and solely dependent on their respective decision threshold. Hence we can independently optimize each of the parts as earlier to optimize the overall value of the whole expression (3.1). We find convex region to be

$$(\mu_0^{\mathrm{SR}} - \eta_{\mathrm{R}}) \leq 0 \quad \text{and } (-\mu_1^{\mathrm{SR}} + \eta_{\mathrm{R}}) \leq 0. \tag{3.12}$$

and

$$(\mu_0^{\mathrm{RD}} - \eta_{\mathrm{D}}) \leq 0 \quad \text{and } (-\mu_1^{\mathrm{RD}} + \eta_{\mathrm{D}}) \leq 0. \tag{3.13}$$

Since the convex region of joint optimization is similar to the problem earlier, we apply our approach to each of the above-stated parts. The results of joint optimization are illustrated in Fig. 4.5.

3.3 Optimization of Relay Location and Messenger Molecules Distribution Parameter

To optimize the relay positioning and messenger molecules distribution, we use Block Coordinate Descent Algorithm (BCDA). BCDA is especially useful in optimization of two parameters where the convex region is quite complicated to determine. In BCDA, we iteratively optimize a particular parameter, while the other parameters are set at their latest determined optimal value. Since we aim at optimizing the relay position and the distribution of messenger molecules, we introduce two parameters m and n, to simplify the optimization problem. Parameter m is used for positioning of the relay in the channel and n is for the distribution messenger molecules, by introducing these two parameters we have two variables instead of four.

$$d_{sr} = m \times d \tag{3.14}$$

$$d_{rd} = (1 - m) \times d \tag{3.15}$$

$$N_A = n \times N_T \tag{3.16}$$

$$N_B = (1 - n) \times N_T \tag{3.17}$$

Here, the total channel length and total number of transmitted molecules are given by d and N_T respectively, and our current objective to minimize error can be restated as

$$\min_{m,n} \quad P_e[j] \tag{3.18}$$

The BCDA is based on the idea of fixing all the variables except for one and finding the optimal value of this variable that minimizes the objective function. This process is iterated over all the variables until convergence. The convergence is achieved if there exists a single solution that minimizes the objective function at each iteration which optimizes one variable. In the following, we show that the error function (3.1) is quasiconvex for each variable (m and n) while the other variable is fixed. Thus, the proposed iterative algorithm based on the BCDA converges to the optimal solution independent of the initial value at which the algorithm starts.

By applying the BCDA algorithm, we first consider the problem for the fixed value of n as follows:

$$\min_{m} \quad P_e[j] \tag{3.19}$$

Since taking the second derivative of the objective function (3.1), P_e, with respect to the relay position, m, is very difficult, we determine its convexity (or concavity). By verifying its behavior with respect to m in Chapter 4. In Fig. 4.6-4.7, we reveal that the bit error probability

function P_e with respect to the relay position when the destination decision threshold is fixed, is quasiconvex since its domain and all sublevel sets are convex. Thus, the optimization problem (3.19) to find the optimum relay position, m^{opt}, is a quasiconvex problem.

In the next step of the BCDA algorithm, we fix the value of m, and then find the optimal value of n that minimizes the given objective function i.e.,

$$\min_{n} \quad P_e[j] \tag{3.20}$$

The second derivative of the objective function with respect to the messenger molecules distribution parameter (n) is also complex. Hence we prove it's convexity similar to the parameter m . Both the quasiconvex optimization problem can be solved by the bisection method explained in Algorithm 1 .

Algorithm 1 Bisection Method

Initialization:
Set $0 < \epsilon < 1$, $l \leq P_e[p = p^*] \leq u$ ($l = 0$ and $u = 1$).
Iterations:
Step 1: $\alpha := (l + u)/2$
Step 2: Solve the convex feasibility problem (3.21)
Step 3: If feasible then set $u := \alpha$ or else $l := \alpha$
Until $\| u - l \| \leq \epsilon$

The convex feasibility at each iteration can be expressed as:

$$\begin{aligned} &\text{Find} \quad p \\ &\text{s.t.} \quad P_e[j] - \alpha \leqslant 0 \end{aligned} \tag{3.21}$$

where p is the parameter to be optimized and $\alpha \in \mathbb{R}$. After finding the values of m and n, the aforementioned steps are repeated until these values converge [25]. These steps for solving the optimization problem (3.18) are described by an iterative algorithm based on the BCDA presented in Algorithm 2.

Algorithm 2 BCDA for joint optimization of m and n

Initialization:
Set $0 < \epsilon < 1$ and iteration number $q := 0$, for arbitrary value of n^0
find m^0 in (3.19) by the bisection method, for $n = n^0$.
Iterations:
Step 1: For fixed m^q; find n^{q+1} in (3.20) by bisection method in Algorithm 1
Step 2: For fixed n^{q+1}; find m^{q+1} in (3.19) by bisection method
Step 3: Set $q := q + 1$
Until $\| m^{q+1} - m^q \| \leq \epsilon$ and $\| n^{q+1} - n^q \| \leq \epsilon$

The solution using BCDA is illustrated in Fig.4.10 of Chapter 4.

Chapter 4

Numerical and Simulation Results

In this section, we evaluate the error performance of the considered DbMC system using Monte Carlo simulation approach (as in [26]) with fixed transmitter location and realization of Gaussian distributed noisy molecular observations whose statistics are provided in Chapter 3. For all the sections in this chapter, We consider information-carrying molecules of radius 2.56 nm (e.g., human insulin hormone molecules) in a diffusive medium (e.g., blood) having uniform viscosity of 10^{-3} kg $\mathrm{m}^{-1}\mathrm{s}^{-1}$ at a temperature of 310 °K [18], [19]. We choose value of several parameters from [19] as $d = 10$ μm, $r = 10$ μm, $D_A = D_B = 79.4$ $\mu\mathrm{m}^2\mathrm{s}^{-1}$, $\lambda = 5.41$ s^{-1}, and $T = 0.2$ s. Furthermore, we select $N_T = 800$, $\mu_{\mathrm{no}}^{\mathrm{SR}} = \mu_{\mathrm{no}}^{\mathrm{RD}} = \sigma_{\mathrm{no}}^{2,\mathrm{SR}} = \sigma_{\mathrm{no}}^{2,\mathrm{RD}} = 50$ and $I = 10$.

4.1 Decision Thresholds

First, we illustrate the effectiveness of our optimization solution in terms of accuracy and convergence time and calculating the detection threshold at node R using ML principle. Since the distribution of allocated molecules and the position of relay is fixed in this case, $N_A = N_B = 400$ and $d_{\mathrm{SR}} = d_{\mathrm{RD}} = 10$ μm. Simulation results are obtained by averaging over 10^4 random realizations of the observations. In Fig. 4.1, the error probability of considered DbMC system is evaluated as a function of detection threshold η_{D} to show the relative placement of our optimization solution, $\eta_{\mathrm{D}}^{\mathrm{opt}}$, with respect to the optimal point on the error curve. One can clearly see that $\eta_{\mathrm{D}}^{\mathrm{opt}}$ coincides with the minimum error point of $P_e[j]$. Moreover, analytical result matches well with the simulation points. Fig. 4.1 also illustrates the central path associated with problem (3.9). The central path comprises of central or suboptimal points $\eta_{\mathrm{D}}^{\mathrm{Sopt}}$, given by (3.8). We compute $\eta_{\mathrm{D}}^{\mathrm{Sopt}}$ for a sequence of increasing value of ε, until $\varepsilon \geq (2/tolerance)$, which guarantees optimal solution within the *tolerance*. One can observe the shifting of $\eta_{\mathrm{D}}^{\mathrm{Sopt}}$ towards $\eta_{\mathrm{D}}^{\mathrm{opt}}$ as ε grows.

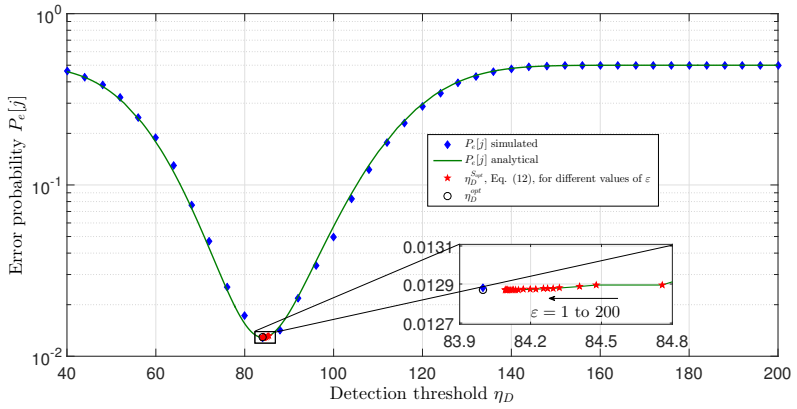

FIGURE 4.1: $P_e[j]$ and central points $\eta_{\mathrm{D}}^{\mathrm{Sopt}}$ as a function of η_{D} and ε respectively.

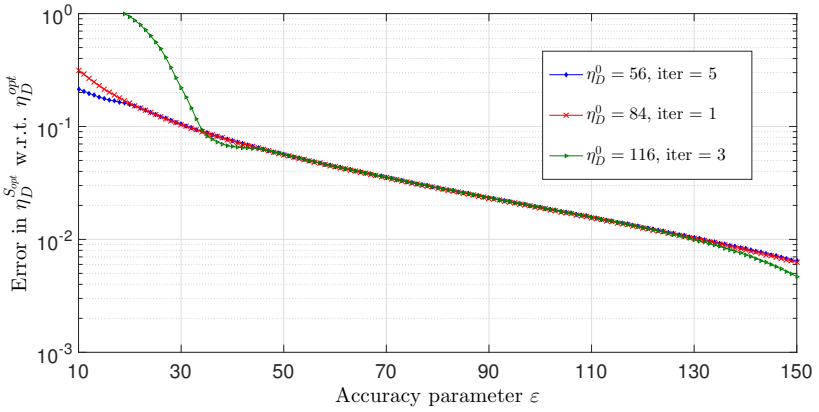

FIGURE 4.2: Error in suboptimal detection thresholds $\eta_{\mathrm{D}}^{\mathrm{Sopt}}$ as a function of ε.

Fig. 4.2 shows the error in $\eta_{\mathrm{D}}^{\mathrm{Sopt}}$ with respect to $\eta_{\mathrm{D}}^{\mathrm{opt}}$ as a function of ε for different values of initial guess η_{D}^{0} and Newton Raphson iterations. For selected set of parameter values, we obtain $\eta_{opt} = 84$ and consider three (two extreme and one in-between) initial guesses within constraint (3.3) as $\eta_{\mathrm{D}}^{0} = \{56, 84, 116\}$. One can clearly see that the error associated with $\eta_{\mathrm{D}}^{\mathrm{Sopt}}$ decreases with increasing value of ε. Hence, the ε plays a crucial role in deciding optimal solution before rounding operation is applied to get an integer $\eta_{\mathrm{D}}^{\mathrm{opt}}$. Hereby, one should choose an appropriate high value of ε that affects only the fractional part of $\eta_{\mathrm{D}}^{\mathrm{Sopt}}$ so as to ensure optimal threshold when rounding operation is performed. For instance, one can see Fig. 4.1 where increasing value of ε adjusts the fractional part of $\eta_{\mathrm{D}}^{\mathrm{Sopt}}$ from a value greater than 0.5 to a value less than 0.5. Consequently, rounding operation provides $\eta_{\mathrm{D}}^{\mathrm{opt}} = round(\eta_{\mathrm{D}}^{\mathrm{Sopt}}) = 84$, instead of 85. Further, one can observe that the value of ε around 130 is sufficiently high for rounding operation to provide optimal threshold for any initial guesses (lying within inequality constraints) in very few iterations.

Fig. 4.3 depicts the optimum detection threshold $\eta_{\mathrm{D}}^{\mathrm{opt}}$ as a function of iterations for different values of initial guess η_{D}^{0} and accuracy parameter ε. One can observe from Fig. 4.2 that the error in $\eta_{\mathrm{D}}^{\mathrm{Sopt}}$ is more than 0.1 for $\varepsilon = 20$, hence more iterations (1 to 5), prior to the rounding

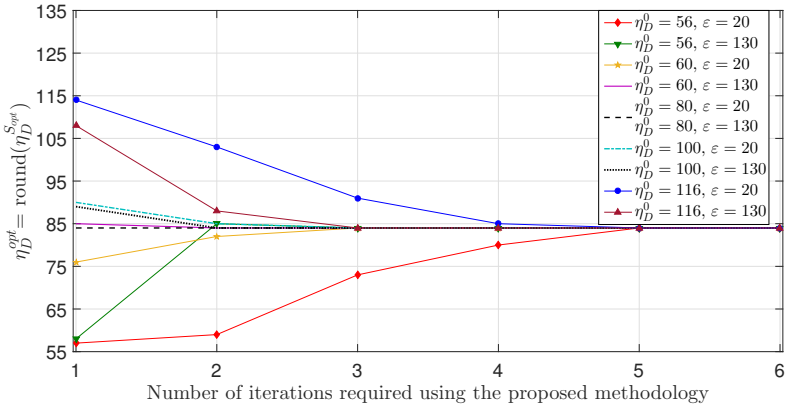

FIGURE 4.3: $\eta_{\mathrm{D}}^{\mathrm{opt}}$ as a function of iterations required using proposed methodology.

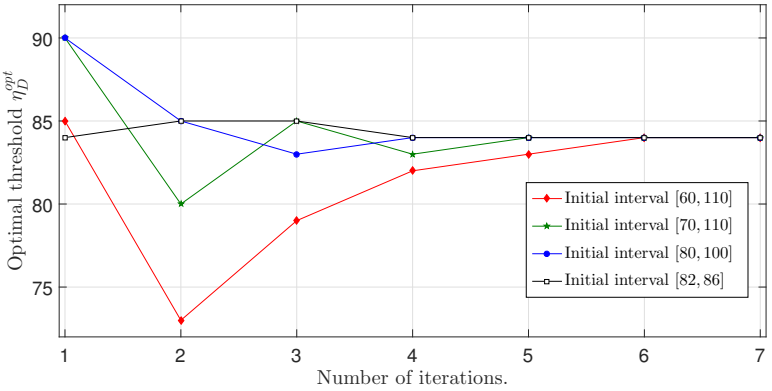

FIGURE 4.4: $\eta_{\mathrm{D}}^{\mathrm{opt}}$ as a function of iterations required using methodology in [13].

operation, are required to yield $\eta_{\mathrm{D}}^{\mathrm{opt}}$ as depicted in Fig. 4.3. However only 1 to 3 iterations are required to achieve $\eta_{\mathrm{D}}^{\mathrm{opt}}$, using $\varepsilon = 130$ (suggested through the explanation of Fig. 4.2, corresponding to the error of 0.01), for any initial guesses lying within the inequality constraints. Moreover, for comparison purpose, using the same *tolerance* of 0.01, we also plot Fig. 4.4 for optimization methodology proposed in [13] using bisection method for various initial intervals containing the optimal threshold. One can clearly see from Figs. 4.3 and 4.4 that our proposed methodology provides optimal solution comparatively in less iterations. This is because, unlike the slow convergence of Bisection method owing to its dependence on the size of initial interval, accuracy parameter ε along with Newton Raphson method helps in the quick convergence of $\eta_{\mathrm{D}}^{\mathrm{s_{opt}}}$.

Fig. 4.5 depicts the error probability of considered DbMC system as a function of both the detection thresholds. One can clearly see that the minimal in the three-dimensional plot coincides with both the optimal thresholds, $\eta_{\mathrm{R}}^{\mathrm{opt}}$ and $\eta_{\mathrm{D}}^{\mathrm{opt}}$. It is clear from the figure that the whole system can be split into two independent links and separately optimized.

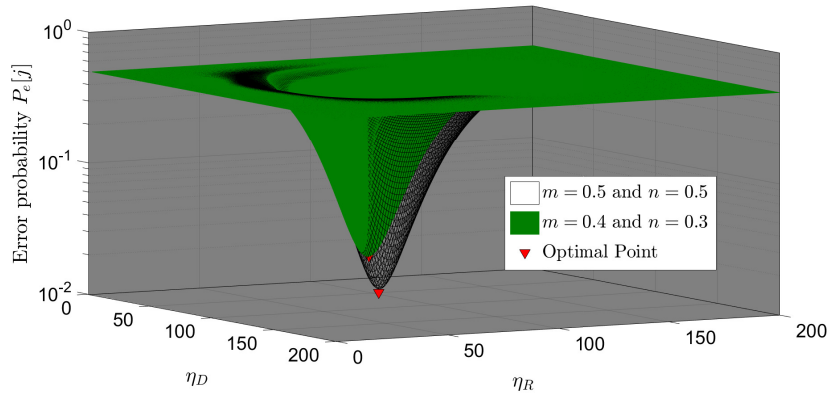

FIGURE 4.5: $P_e[j]$ versus the decision threshold η_{R} at relay node and decision threshold η_{D} at destination node

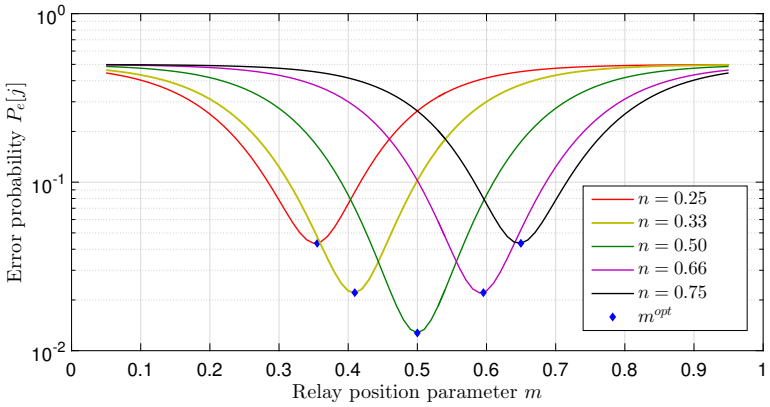

FIGURE 4.6: $P_e[j]$ versus the location of the relay node with fixed decision threshold ($\eta_{\mathrm{R}} = \eta_{\mathrm{D}} = 84$).

4.2 Relay Positioning and Distribution of Messenger Molecules

In this case, as mentioned in the previous chapter, the decision thresholds are fixed. First, we prove the concave (convex) nature of each of the parameters individually for which we make use of Algorithm 1, after we prove them to be quasiconvex, we use BCDA mentioned in Algorithm 2 (Note: For Algorithms 1 and 2, $\epsilon = 0.0001$). In Fig. 4.6, the error probability performance of the network is plotted against the relay location parameter (m) for different values of messenger molecules distribution parameter (n). Since the detection thresholds are fixed we plot these curves for $\eta_{\mathrm{R}} = \eta_{\mathrm{R}} = 84$. We also evaluate the performance of the proposed algorithm to find the optimal value of the relay location in Fig. 4.6. The total number of messenger molecules of types A and B in the network is assumed to be fixed ($N_T = 800$). We consider five different cases and observe that in each case, there is an optimum value of m that minimizes the network error. It is also observed that the optimum value of m depends on the values of N_A and N_B,

Likewise, we also evaluate the proposed algorithm for fixed values of $N_A = N_B = 400$ and for varying values of detection thresholds (η_{R} and η_{D}). It is clear from both the figures that the error

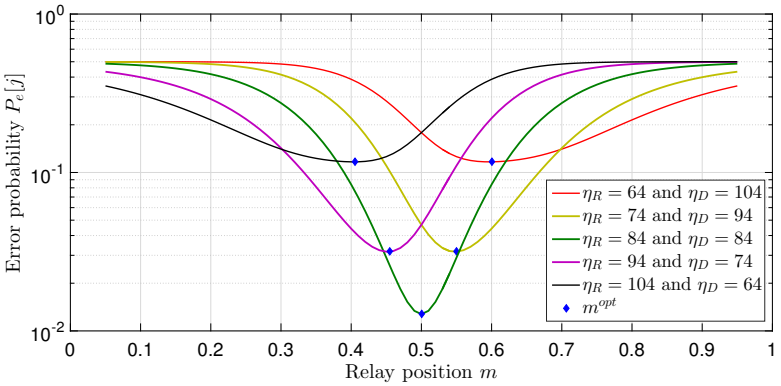

FIGURE 4.7: $P_e[j]$ versus the location of the relay node with fixed messenger molecules distribution parameter ($n = 0.5$).

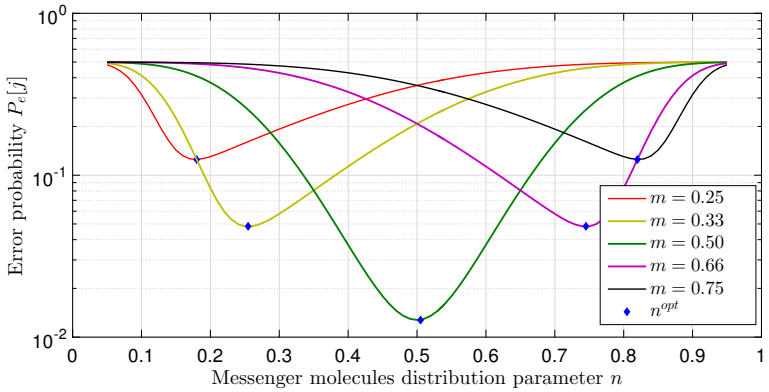

FIGURE 4.8: $P_e[j]$ versus the messenger molecules distribution parameter with fixed decision thresholds ($\eta_{\mathrm{R}} = \eta_{\mathrm{D}} = 84$).

probability as a function of the relay position is a quasiconvex function due to the convexity of its domain and sublevel sets. Thus, by using the Bisection method global optimum relay position can be accurately found.

Similarly in Fig. 4.8 and Fig. 4.9, the error probability performance of the network is plotted against the message molecules distribution parameter (n) for different values of relay distance (m) and detection thresholds (η_{R} and η_{D}). In Fig. 4.8, the detection thresholds are fixed, $\eta_{\mathrm{R}} = \eta_{\mathrm{R}} = 84$, and m is varied. In Fig. 4.9, the relay is fixed at the center ($m = 0.5$) and the detection thresholds are varied. It is clear from both the figures that the error probability as a function of messenger molecules distribution parameter (n) is also a quasiconvex function.

Since we have established the quasiconvex nature of error probability with respect to m and n, we can apply BCDA to these two parameters to find their optimal value for a given power and detection threshold constraint. In Fig. 4.10, a three-dimensional plot of error probability against parameters m and n is plotted. Two cases are considered, in the first case $\eta_{\mathrm{R}} = \eta_{\mathrm{D}} = 84$, for the second case $\eta_{\mathrm{R}} = 74$ and $\eta_{\mathrm{D}} = 94$. In both the cases our proposed algorithm based on BCDA,

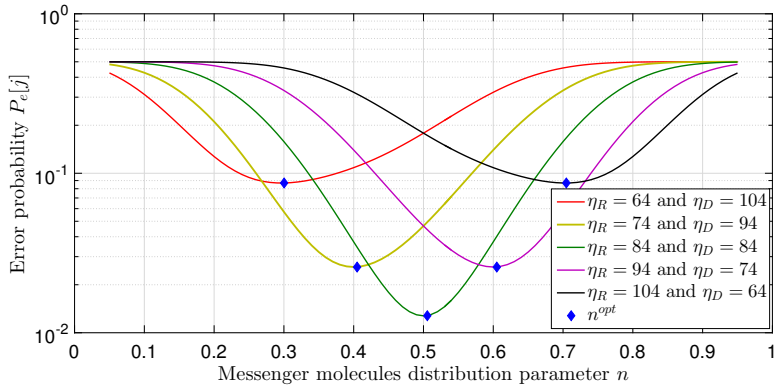

FIGURE 4.9: $P_e[j]$ versus the messenger molecules distribution parameter with fixed relay position ($m = 0.5$).

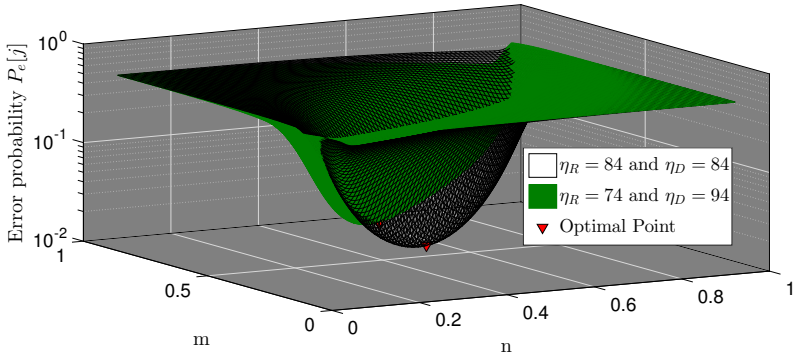

FIGURE 4.10: $P_e[j]$ versus relay position parameter and messenger molecules distribution parameter

discussed in Chapter 3, was able to predict the optimal values of m and n by determining the minimal value of error probability.

Chapter 5

Conclusion

In this report, we considered a relay aided diffusion-based molecular communication system and presented an analytical study on its error probability performance. We derived a closed-form expression for the bit error probability of the network, the derived expression was used to classify two sets of problems for joint optimization. The first problem set was on joint optimization of the decision thresholds at the relay and destination node, we solved it by using logarithmic barrier followed by Karush-Kuhn-Tucker interpretation of the centrality condition and Newton Raphson method. The second problem was relay positioning and messenger molecules distribution optimization problem and we solved it by an iterative-based algorithm. Using numerical results, we proved the efficiency of our proposed method for the first case and the nature of optimization problems (convexity or concavity) for the second case. Finally, we showed that by solving the proposed optimization problems, optimal values of parameters can be jointly obtained.

Bibliography

[1] J. G. Proakis "Digital Communications," Boston, McGraw-Hill, 2001

[2] W. K. Purves, D. Sadava, G. H. Orians, and H. C. Heller, "Life: The Science of Biology," Sinauer Associates, 2001

[3] I. F. Akyildiz, F. Brunetti, and C. Blazquez, "Nanonetworks: A new communication paradigm," *Comput. Netw.*, vol. 52, no. 12, pp. 2260–2279, May 2008.

[4] T. Nakano, M. J. Moore, F. Wei, A. V. Vasilakos, and J. Shuai, "Molecular communication and networking: Opportunities and challenges," *IEEE Trans. NanoBiosci.*, vol. 11, no. 2, pp. 135-148, Jun. 2012.

[5] M. Pierobon and I. F. Akyildiz "A physical end-to-end model for molecular communication in nanonetworks," *IEEE J. Sel. Areas Commun.*, vol. 28, no. 4, pp. 602611, May 2010.

[6] N. Farsad, W. Guo, and A. W. Eckford, "Tabletop molecular communication: text messages through chemical signals," *PLoS ONE*, vol. 8, no. 12, p. e82935, Dec. 2013.

[7] B. Alberts, D. Bray, K. Hopkin, A. Johnson, J. Lewis, M. Ra, K. Roberts, and P. Walter, "Essential Cell Biology," *3rd ed.*, Garland Science, 2010.

[8] L. Hong, W. Chen, and F. Liu, "Cooperative molecular communication for nanonetwork," *Proc. IEEE Int. Conf. Ubiquitous Future Netw. (ICUFN)*, pp. 369-370, Jul. 2014.

[9] A. Ahmadzadeh, A. Noel, and R. Schober, "Amplify-and-forward relaying in two-hop diffusion-based molecular communication networks," *Proc. IEEE Global Commun. Conf. (GLOBECOM)*, pp. 1-7, Dec. 2015.

[10] A. Einolghozati, M. Sardari, and F. Fekri, "Relaying in diffusion-based molecular communication," *Proc. IEEE Int. Symp. Inf. Theory (ISIT)*, pp. 1844-1848, Jul. 2013.

[11] A. Ahmadzadeh, A. Noel, and R. Schober, "Analysis and design of multi-hop diffusion-based molecular communication networks," *IEEE Trans. Mol. Biol. Multi-Scale Commun.*, vol. 1, no. 2, pp. 144-157, Jun. 2015.

[12] A. Noel, K. C. Cheung, and R. Schober, "Optimal receiver design for diffusive molecular communication with flow and additive noise," *IEEE Trans. NanoBiosci.*, vol. 13, no. 3, pp. 350-362, Sep. 2014.

[13] N. Tavakkoli, P. Azmi, and N. Mokari, "Performance evaluation and optimal detection of relay-assisted diffusion-based molecular communication with drift," *IEEE Trans. NanoBiosci.*, vol. 16, no. 1, pp. 34-42, Jan. 2017.

[14] I. Llatser, A. Cabellos-Aparicio, and E. Alarcon, "Networking challenges and principles in diffusion-based molecular communication," *IEEE Wireless Comm.*, vol. 19, no. 5, pp. 36-41, Oct. 2012.

[15] A. Noel, K. C. Cheung, and R. Schober, "Improving diffusion-based molecular communication with unanchored enzymes," *IEEE Wireless Comm.*, vol. 19, no. 5, pp. 36-41, Oct. 2012.

[16] B. Atakan O. B. Akan and S. Balasubramaniam, "Body area nanonetworks with molecular communications in nanomedicine," *IEEE Commun. Mag.*, vol. 50, no. 1, pp. 28-34, Jan. 2012.

[17] H. B. Yilmaz, A. C. Heren, T. Tugcu, and C.-B. Chae, "Target detection and tracking by bionanosensor networks," *SpringerBriefs in Computer Science*, 2016.

[18] H. B. Yilmaz, A. C. Heren, T. Tugcu, and C.-B. Chae, "Three-dimensional channel characteristics for molecular communications with an absorbing receiver," *IEEE Commun. Lett.*, vol. 18, no. 6, pp. 929-932, Jun. 2014.

[19] A. C. Heren, H. B. Yilmaz, C.-B. Chae, and T. Tugcu, "Effect of degradation in molecular communication: Impairment or enhancement? ," *IEEE Trans. Mol. Biol. Multi-Scale Commun.*, vol. 1, no. 2, pp. 217-229, Jun. 2015.

[20] H. ShahMohammadian, G. G. Messier, and S. Magierowski, "Blind synchronization in diffusion-based molecular communication channels," *IEEE Commun. Lett.*, vol. 17, no. 11, pp. 2156-2159, Nov. 2013.

[21] B. Li, M. Sun, S. Wang, W. Guo, and C. Zhao, "Local convexity inspired low-complexity noncoherent signal detector for nano-scale molecular communications," *IEEE Trans. Commun.*, vol. 64, no. 5, pp. 2079-2091, May 2016.

[22] S. Boyd and L. Vandenberghe, *Convex Optimization*. Cambridge University Press, 2004.

[23] L. Lin, J. Zhang, M. Ma, and H. Yan, "Time synchronization for molecular communication with drift," *IEEE Commun. Lett.*, vol. 21, no. 3, Mar. 2017.

[24] S. K. Tiwari, T. R. T. Reddy, and P. K. Upadhyay, "Error Performance Optimization using Logarithmic Barrier Function in Molecular Nanonetworks," *IEEE Commun. Lett.*, vol. 21, no. 11, Nov. 2017.

[25] P. Tseng, "Convergence of a block coordinate descent method for nondifferentiable minimization," *J. Optim. Theory Appl.*, vol. 109, no. 3, pp. 475-494, Jun. 2001.

[26] Y. Deng, A. Noel, W. Guo, A. Nallanathan, and M. Elkashlan, "Analyzing large-scale multiuser molecular communication via 3D stochastic geometry,", arXiv preprint arXiv:1704.06929v2 [cs.IT], May. 2017.